Electronic Supplementary Material (ESI) for Journal of Materials Chemistry A.
This journal is © The Royal Society of Chemistry 2019

Supporting Information

# Host-Guest Interactions of Catechol and 4-Ethylcatechol with Surface-Immobilized Blue-Box Molecules

Ahmed Owais,[a,b] Alex M. Djerdjev,[a] James M. Hook,[c] Alex Yuen,[a] William Rowlands,[d] Nicholas G. White,[e] Chiara Neto[a]*

[a] *School of Chemistry and The University of Sydney Nano Institute, The University of Sydney, NSW 2006 Australia*

[b] *Renewable Energy Science and Engineering Department, Faculty of Postgraduate Studies for Advanced Sciences (PSAS), Beni-Suef University, Beni-Suef 62511, Egypt*

[c] *Mark Wainwright Analytical Centre and School of Chemistry, University of New South Wales, Sydney, NSW, 2052, Australia*

[d] *Licella Pty Ltd, 140 Arthur Street, North Sydney NSW 2060 Australia*

[e] *Research School of Chemistry, The Australian National University, Canberra, ACT, Australia*

## X-ray crystallography

*General remarks*

We grew crystals of 1:1 complexes of $\mathbf{BB^{4+}}$ and catechol from a range of solvents: **BB·4Cl·catechol** by vapour diffusion of diethyl ether into a methanol solution of the components, **BB·4Cl·catechol** by vapour diffusion of acetone into a methanol solution of the components and $\mathbf{BB{\cdot}4PF_6{\cdot}catechol}$ by vapour diffusion of diethyl ether into an acetonitrile solution of the components. In some cases, more than one dataset was collected including using synchrotron radiation. Typically, crystals diffracted well, and high-quality diffraction data could be obtained.

In all cases, the structure of the macrocycle is clear and typically the anions are also well-defined. In each case, there is an area of electron density within the macrocycle that appears to correspond to a highly disordered catechol molecule (often across a symmetry operation), an example of this is shown in Fig. S1. In most cases, it was not possible to refine this disordered catechol satisfactorily and so satisfactory refinement of the data was not possible. Similarly, we were able to obtain crystals of the 1:1 complex between $\mathbf{BB{\cdot}4PF_6}$ and either 2-hydroxyaniline or 3-hydroxyaniline (both from vapour diffusion of diethyl ether into a solution of the components in acetonitrile), but had similar problems. This type of crystallographic disorder has been previously observed in the complex of $\mathbf{BB{\cdot}4PF_6}$ and 1,2-dimethoxybenzene.[1]

In the case of **BB·4Cl·catechol** grown by vapour diffusion of diethyl ether into a methanol solution of the components, a refinement was achieved, although the disordered catechol guest is still only poorly-defined and has large thermal ellipsoids.

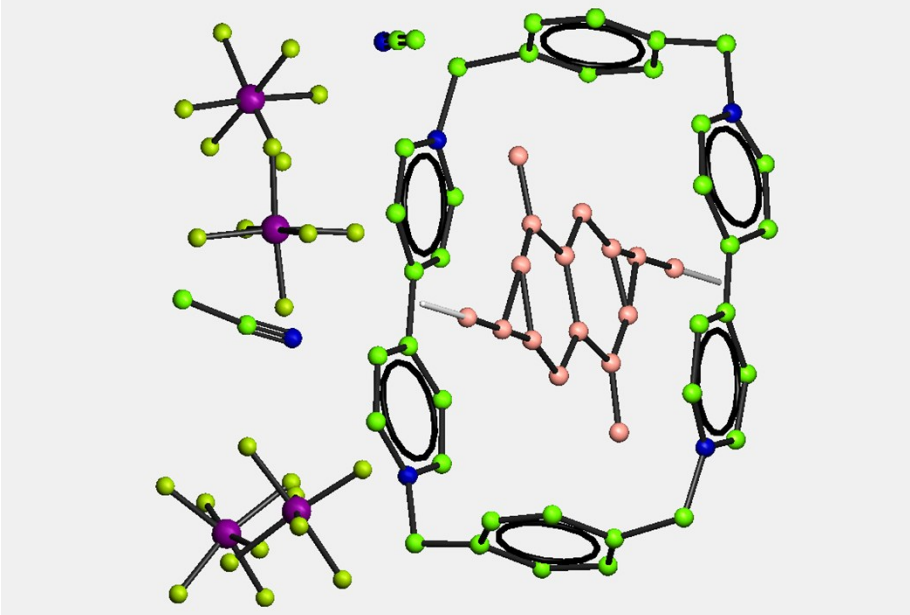

**Fig. S1:** Partially-refined X-ray crystal structure of **BB·4PF$_6$·catechol** grown by vapour diffusion of diethyl ether into an acetonitrile solution of the components. Q-peaks are shown as pink spheres. It was not possible to satisfactorily model the disordered guest, despite numerous attempts.

*Structure of **BB·4Cl·catechol***

Single crystals (red blocks) were obtained by the diffusion of diethyl ether vapour into a methanol solution containing a 1:1 mixture of **BB·4Cl** and catechol. Data were collected using mirror-monochromated Cu Kα radiation on an Agilent SuperNova diffractometer. The crystal was cooled to 150 K using a Cryostream $N_2$ open-flow cooling device[2] in all cases. Raw frame data (including data reduction, interframe scaling, unit cell refinement and absorption corrections) were processed using CrysAlisPro.[3] The structure was solved with SIR92 [4] and refined using full-matrix least-squares on $F^2$ within the CRYSTALS suite.[5] All non-hydrogen atoms were refined with anisotropic displacement parameters. C–H hydrogen atoms were generally visible in the Fourier difference map, and were initially refined with restraints on bond lengths and angles, after which the positions were used as the basis for a riding model.[6] Methanol O–H hydrogen atoms were generally visible in the Fourier difference map and their positions were refined with restraints on bond lengths and angles. Due to the disorder involving the catechol group, catechol O–H hydrogen atoms were inserted at calculated positions and these positions used as the basis for a riding model.

The structure crystallises in the centrosymmetric space group P-1, with the centre of inversion located in the centre of the **BB**$^{4+}$ macrocycle (where the disordered catechol resides). Due to the difficulties of refining a highly disordered group across a centre of symmetry, the structure was refined in the non-centrosymmetric space group P1. The catechol group was modelled as disordered over two positions (s.o.f.: 0.50:0.50) and it was necessary to add restraints to the bond lengths and angles of the catechol group, as well its thermal and vibrational ellipsoid parameters to achieve a sensible refinement. Restraints were also added to the methanol C–O bond lengths. Even with the restraints on the catechol group, this still has large ellipsoids, probably indicating further positional disorder. Despite numerous attempts, it was not possible to model this further.

An ellipsoid plot of the structure is given in Fig. S2, and crystallographic data are provided in Table S1. Full crystallographic data in CIF format are provided as Supporting Information (CCDC Number: 1886022).

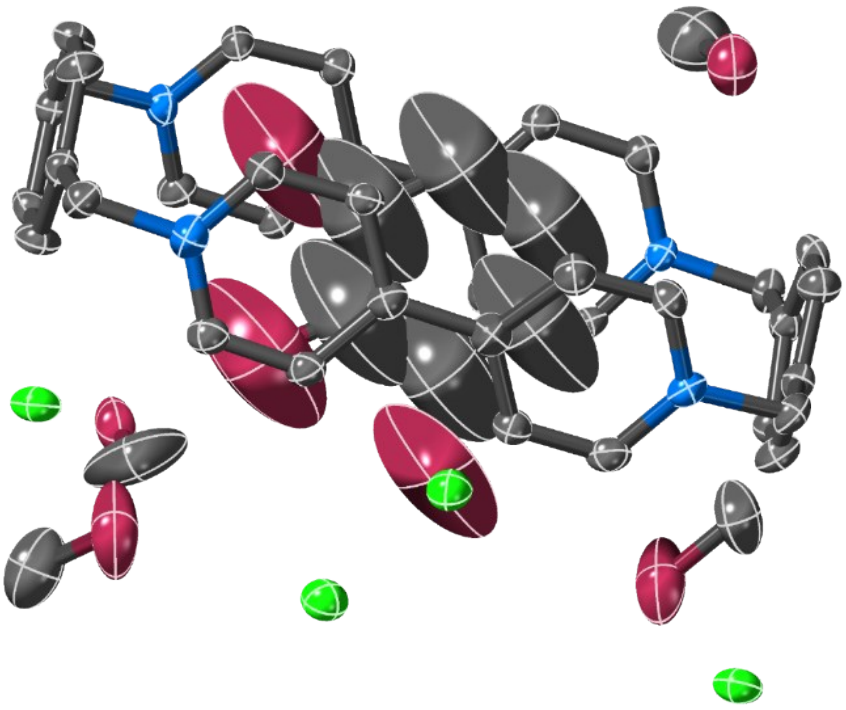

**Fig. S2.** Thermal ellipsoid plot of **BB·4Cl·catechol**, ellipsoids are shown at 50% probability level.

**Table S1.** Selected crystallographic data.

| **Compound** | **BB·4Cl·catechol** |
|---|---|
| Formula | $C_{36}H_{32}N_4 \cdot C_6H_6O_2 \cdot 4(CH_4O) \cdot 4Cl$ |
| Formula weight | 900.77 |
| *a* (Å) | 9.6750(3) |
| *b* (Å) | 10.7761(4) |
| *c* (Å) | 12.8860(4) |
| $\alpha$ (º) | 101.486(3) |
| $\beta$ (º) | 100.639(3) |
| $\gamma$ (º) | 112.862(3) |
| Unit cell volume (Å$^3$) | 1160.97(8) |
| Crystal system | triclinic |
| Space group | *P1* [a] |
| *Z* | 1 |
| Reflections (all) | 22221 |
| Reflections (unique) | 4671 |
| $R_{int}$ | 0.044 |
| $R_1$ [$I > 2\sigma(I)$] | 0.070 |
| $wR_2(F^2)$ (all data) | 0.212 |

[a] The structure crystallises in the space group *P-1*, but was refined in *P1* to make dealing with the catechol group that is disordered about the centre of inversion easier.

**Stability testing**

A 2.0 mM stock solution of **BB·4Cl** in was prepared. Aliquots (0.50 mL) of this were added to solid $K_2CO_3$ (5 mg, 1 wt. %, ~ 36 equiv., pH ~ 11), TBA·F trihydrate (5 mg, 1 wt. %, ~ 16 equiv.), or catechol (0.11 mg, 1.0 equiv.). To another 0.50 mL aliquot was added glacial acetic acid (5 µL, 1%, ~ equiv, pH ~ 3), and another control aliquot was taken without any addition.

All samples were stood at room temperature in capped NMR tubes for 16 hours, then analysed by $^1$H NMR spectroscopy. After this time, the same samples were heated to 80 C for 60 hours and then again analysed by $^1$H NMR spectroscopy.

As can be seen in Figure S3, the macrocycle is stable to a range of stimuli at room temperature over moderate timeframes: none of the added guests caused appreciable decomposition at room temperature over the 16-hour time period. In the presence of base (TBA·F or $K_2CO_3$), H/D exchange with the $D_2O$ solvent is observed resulting in the weakening/disappearance of peaks adjacent to the pyridinium nitrogen atoms (*i.e.* proton c in Figure S3). Catechol causes changes in the peak positions of $\mathbf{BB^{4+}}$, due to the formation of a host–guest complex.

Upon heating, the solution of **BB·4Cl** and $K_2CO_3$ rapidly changed colour, initially forming a blue-green solution, which turned into a colourless solution containing a brown precipitate. While the macrocycle is clearly not stable to heating in basic media, it otherwise appears to be stable with no significant decomposition observed in acidic or neutral solution even after heating for a prolonged period. Remarkably, even in the presence of a large excess of nucleophilic fluoride anions, the macrocycle remains stable. Significant H/D exchange is observed in all samples except for the acidic sample (Figure S4).

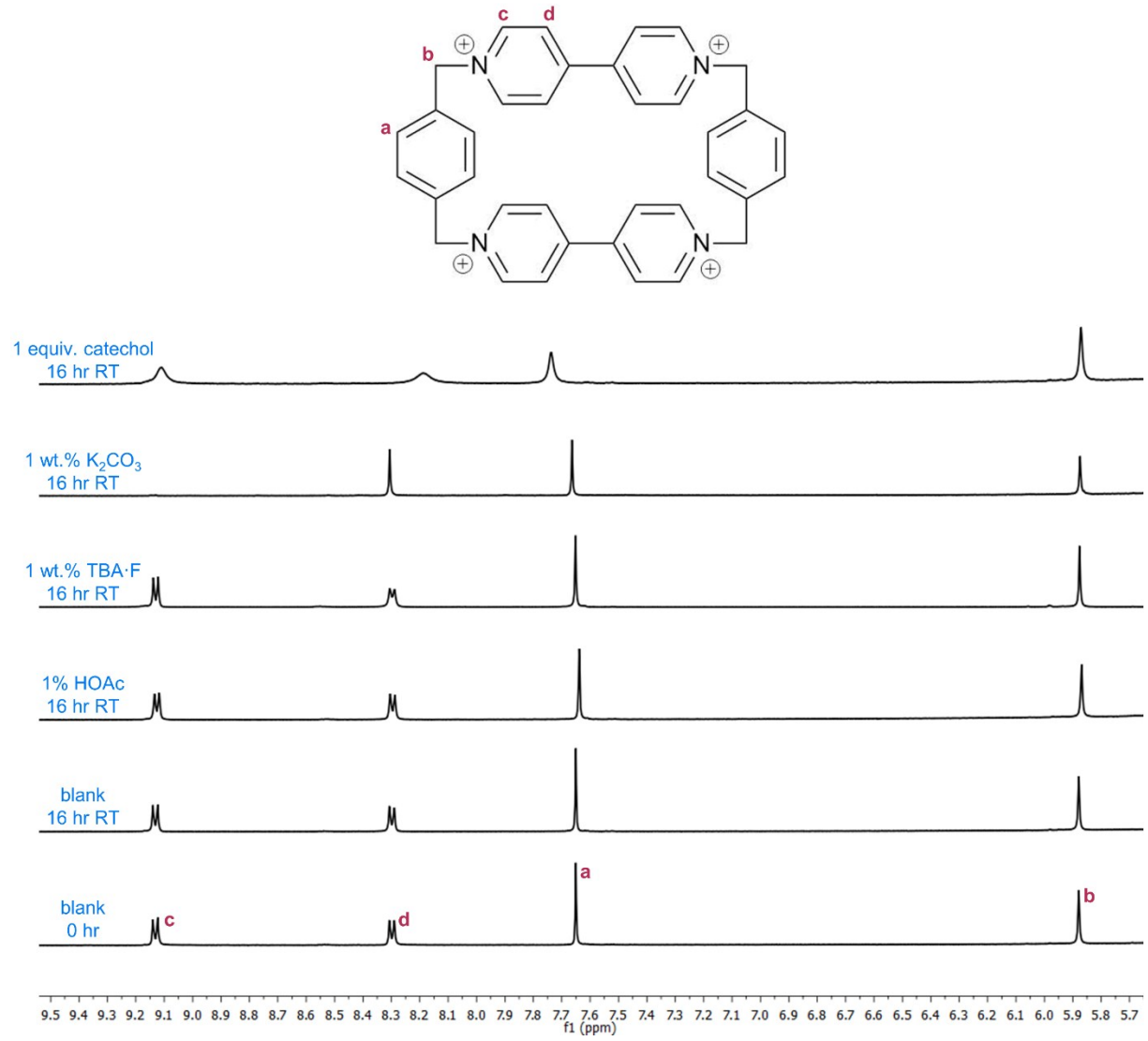


**Figure S3**. Truncated $^{1}$H NMR spectra of **BB·4Cl** in the presence of various stimuli after 16 hours at room temperature (2.0 mM, 298 K, 400 MHz, $D_2O$).

**Figure S4**. Truncated $^{1}$H NMR spectra of BB·4Cl in the presence of various stimuli after 24 hours at room temperature followed by 60 hours at 80 ºC (2.0 mM, 298 K, 400 MHz, $D_2O$).

**Guest binding studies in water**

*UV-Vis titration experiments*

A 0.20 mM solution of **BB·4Cl** in $H_2O$ was prepared and 3.0 mL of this solution placed in a cuvette. Aliquots of a 20 mM solution of guest containing 0.20 mM **BB·4Cl** (to keep the concentration of **BB·4Cl** constant throughout the experiment) were added. The absorbance of the charge-transfer band was monitored and fitted to a 1:1 binding isotherm using the *Bindfit* programme.[7] UV-Vis spectra are provided in Fig. S5–S7

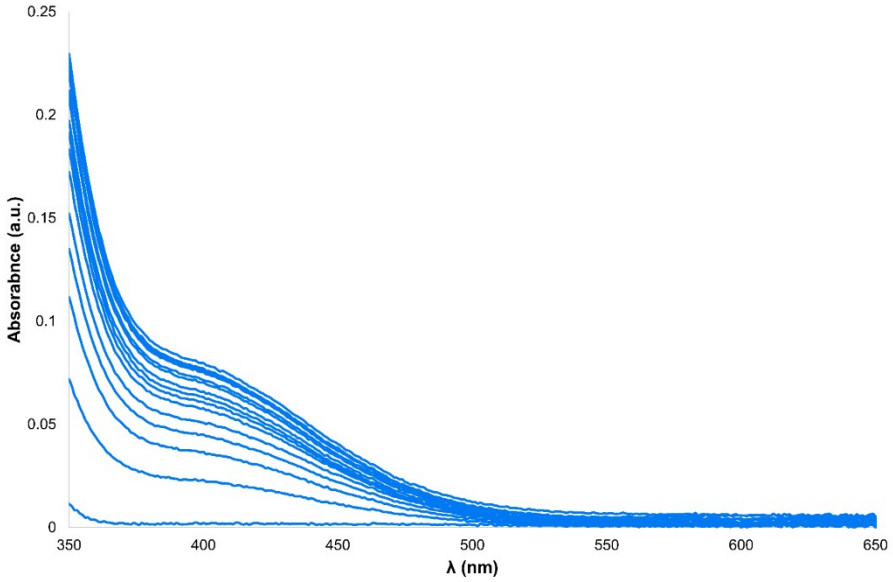


**Fig. S5**. UV-Vis spectra of **BB·4Cl** upon increasing amounts of phenol (water, 298 K). Curves correspond to 0, 0.5, 1.0, 1.5, 2.0, 3.0, 4.0, 5.0, 6.0, 7.0, 10, 20, 25, 30 and 40 equivalents of phenol.

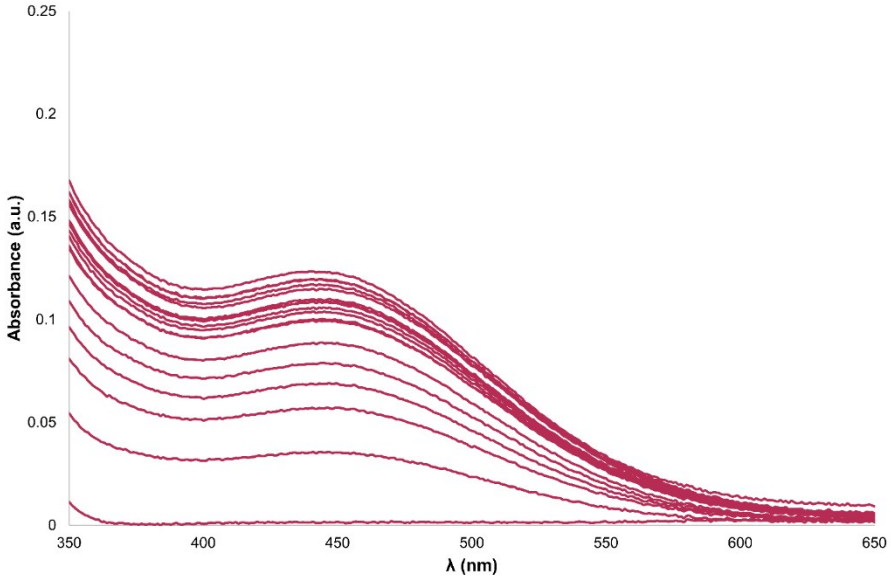


**Fig. S6**. UV-Vis spectra of **BB·4Cl** upon increasing amounts of catechol (water, 298 K). Curves correspond to 0, 0.5, 1.0, 1.5, 2.0, 3.0, 4.0, 5.0, 6.0, 7.0, 8.0, 9.0, 10, 15, 20, 25, 30 and 40 equivalents of catechol.

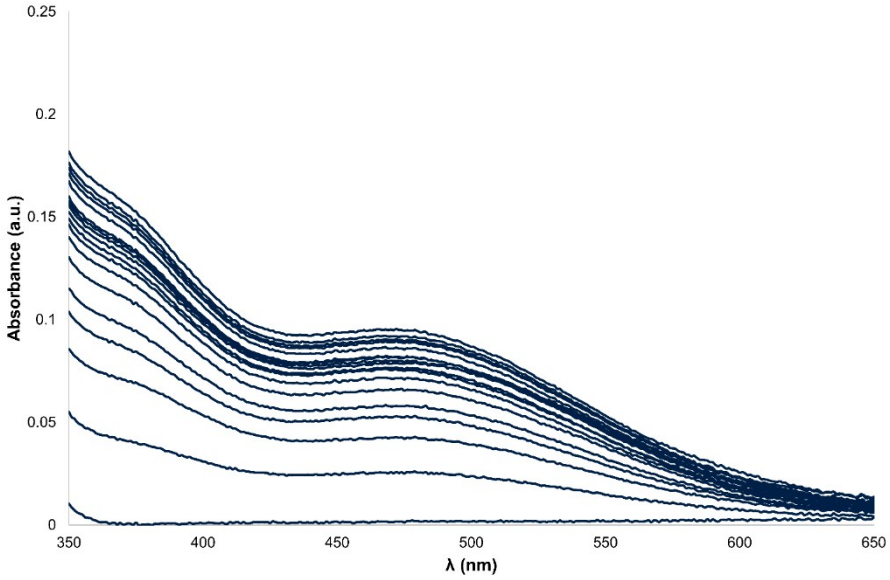


**Fig. S7**. UV-Vis spectra of **BB·4Cl** upon increasing amounts of 4-ethylcatechol (water, 298 K). Curves correspond to 0, 0.5, 1.0, 1.5, 2.0, 3.0, 4.0, 5.0, 6.0, 7.0, 8.0, 9.0, 10, 15, 20, 25, 30 and 40 equivalents of 4-ethylcatechol.

*$^1$H-NMR experiments*

A 2.0 mM solution of **BB·4Cl** in $D_2O$ was prepared, and aliquots of a 100 mM solution of guests in $D_2O$ added. In all cases, resonance (a) moved downfield on addition of the guest, while resonance (d) moved upfield (see Fig. S8–S10 for peak assignment).

**Table S2.** Shift of $BB^{4+}$ resonances on addition of guests (2.0 mM, 298 K, $D_2O$).

| **Guest** | ***Δa*** **(ppm)** | ***Δd*** **(ppm)** |
|---|---|---|
| Phenol, 1.0 equiv. | +0.182 | –0.189 |
| Phenol, 2.0 equiv. | +0.200 | –0.212 |
| Catechol,1.0 equiv. | +0.162 | –0.206 |
| Catechol, 2.0 equiv. | +0.180 | –0.238 |
| 4-Ethylcatechol, 1.0 equiv. | +0.171 | –0.172 |

| | | |
|---|---|---|
| 4-Ethylcatechol, 2.0 equiv. | +0.192 | –0.198 |

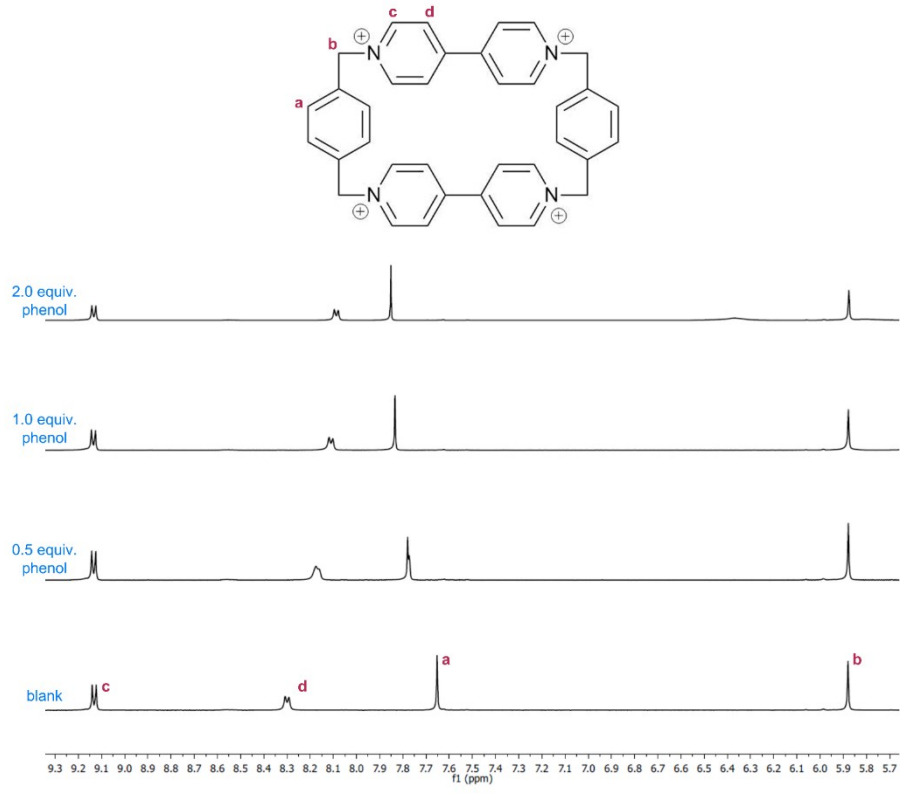


**Fig. S8**. Truncated $^{1}$H NMR spectra of **BB·4Cl** upon addition of phenol (298 K, 400 MHz, $D_2O$, 2.0 mM in **BB·4Cl**).

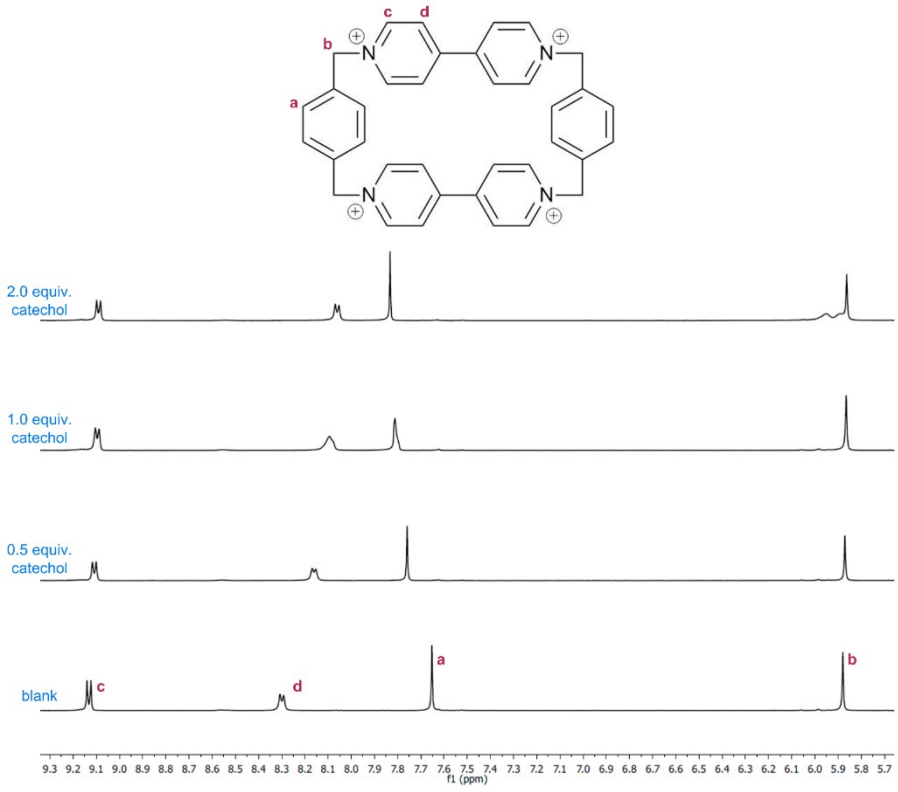


**Fig. S9**. Truncated $^{1}$H NMR spectra of **BB·4Cl** upon addition of catechol (298 K, 400 MHz, $D_2O$, 2.0 mM in **BB·4Cl**).

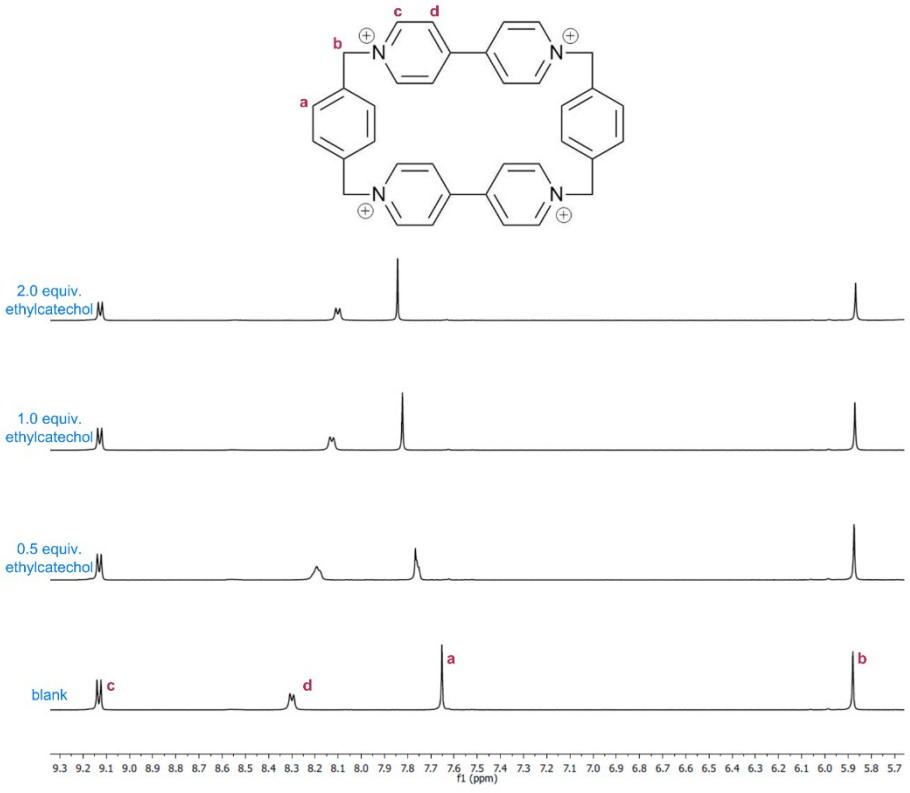


**Fig. S10**. Truncated $^{1}$H NMR spectra of **BB·4Cl** upon addition of 4-ethylcatechol (298 K, 400 MHz, $D_2O$, 2.0 mM in **BB·4Cl**).

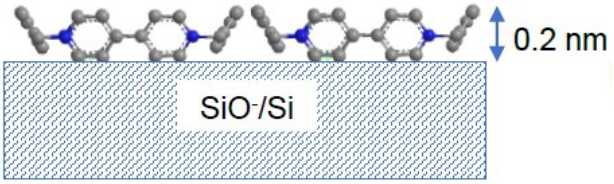


**Fig. S11:** The suggested conformation of BB molecules on silica surfaces.

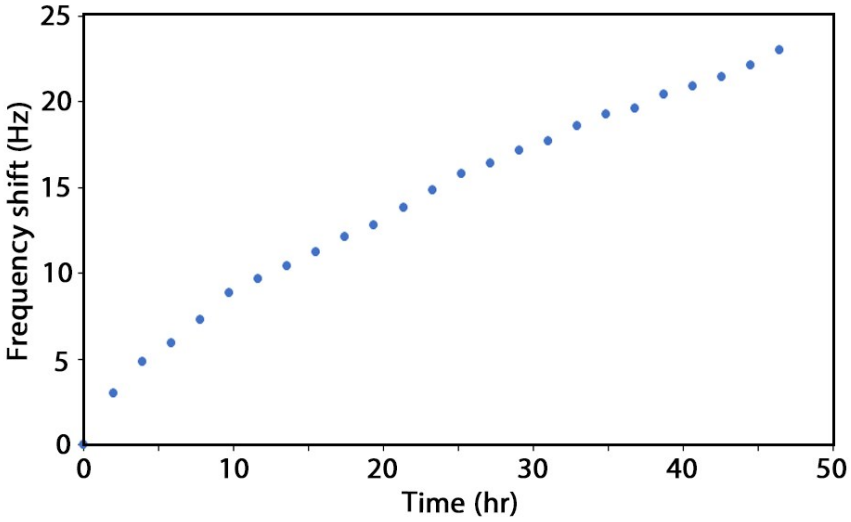


**Fig. S12:** Injection of catechol solutions (4 mM) on bare silicon Q-Sensor as monitored by QCM-D. The data shows no negative frequency shift corresponding to no adsorption of catechol molecules on silica surfaces. The frequency shift is due to a drift in frequency over time (0.2 Hz per 5 min at room temperature).

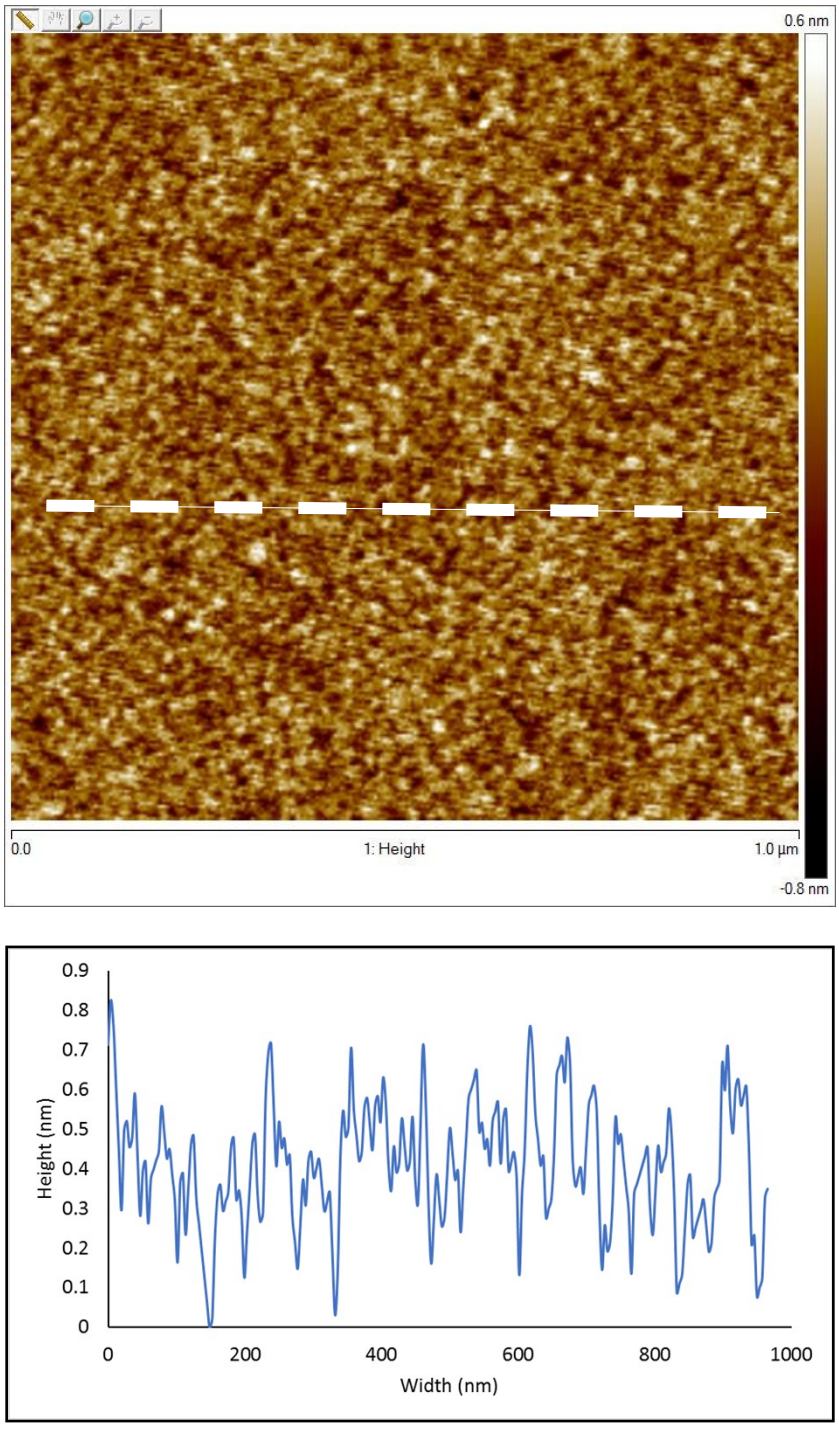


**Fig. S13:** AFM micrographs with the corresponding cross-section profile of BB-coated Si surfaces.

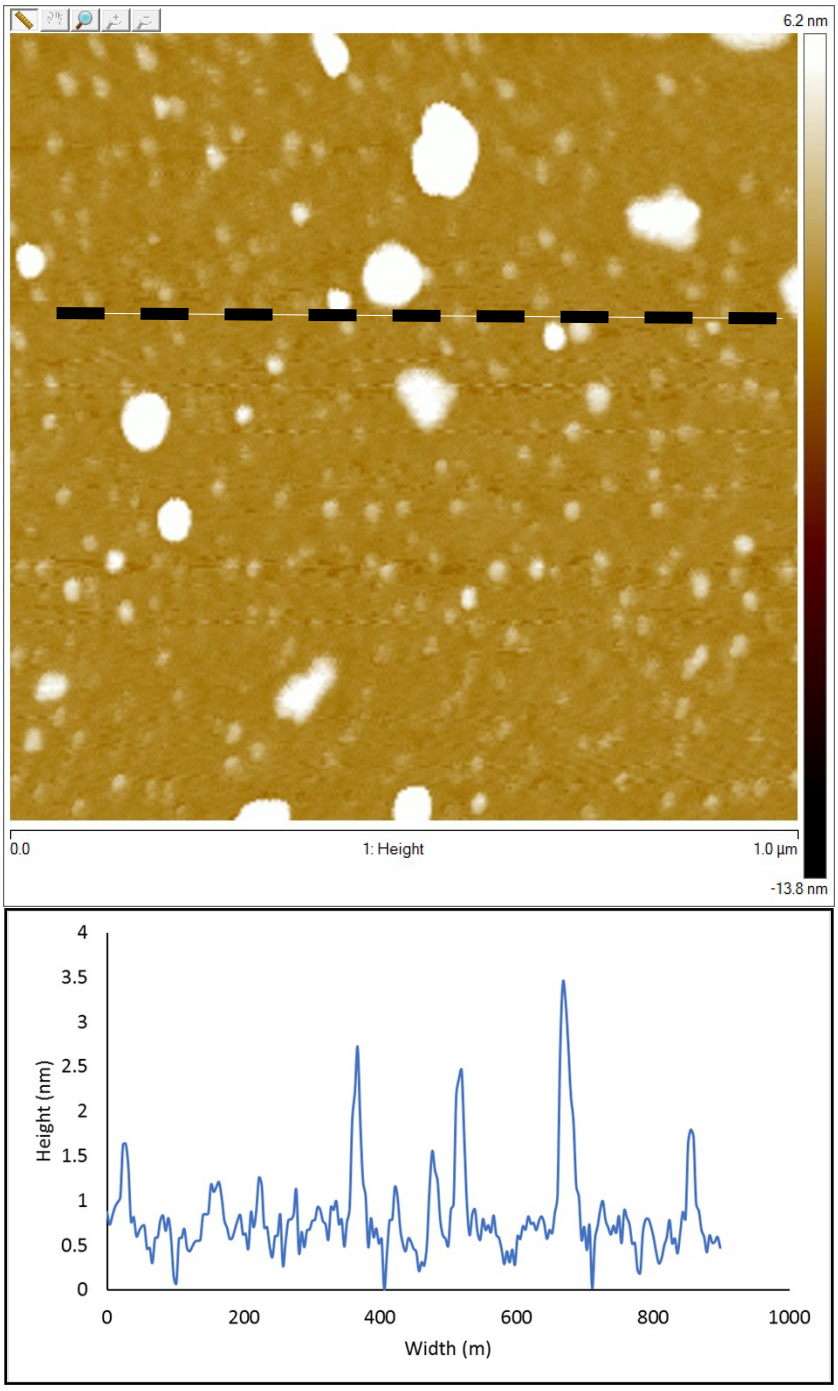


**Fig. S14:** AFM micrographs with the corresponding cross-section profile of BB-coated Si surfaces after immersion in phenol solutions in PBS at pH 7 for 24 hours. Surface roughness (RMS) = 2.5 nm.

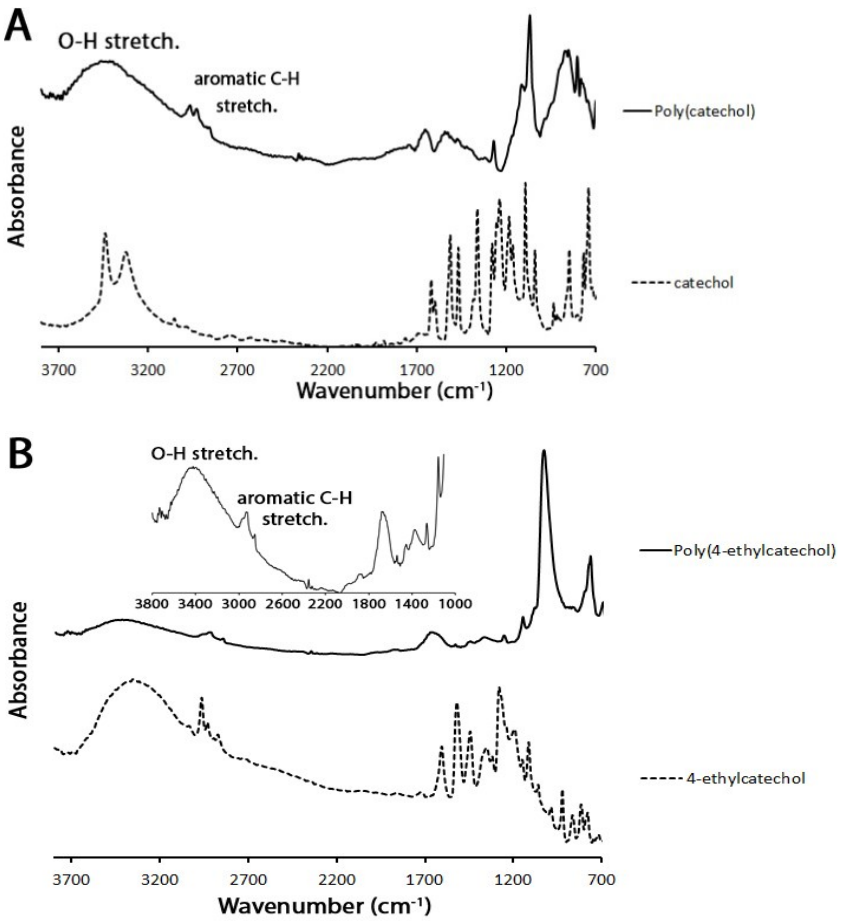


**Fig. S15:** Full FTIR absorption spectra of BB-coated silica surfaces after immersion in A: catechol, B: 4-ethylcatechol solutions after 4 hours. The samples were dried under vacuum over night before the characterisation. The collected absorption data are subtracted from absorption data of the as-received $SiO_2$ powder.

**Recovery of catechol and $BB^{4+}$ from silica**

An 8.5 g sample of silica with **BB·4Cl** (containing 6.5 ± 0.3 mg **BB·4Cl**) and polymerised catechol was extracted with a 6:3:1 mixture of methanol:water:saturated $NH_4Cl_{(aq)}$. The solution was taken to dryness *in vacuo* to give a large amount of salt. This was extracted with acetonitrile in the presence of a large amount (~ 1.5 g) of tetrabutylammonium hexafluorophosphate. This extract was taken to dryness *in vacuo* and $^1$H NMR analysis showed it contained $\mathbf{BB^{4+}}$ macrocycle as well as ammonium and tetrabutylammonium salts and small peaks that could not be identified (Fig. S18).

A 10 g sample of silica with **BB·4Cl** (containing 7.7 ± 0.4 mg **BB·4Cl**, ~11 μmol) was also extracted with a 6:3:1 methanol:water:saturated $NH_4Cl_{(aq)}$ solution and all solvents removed *in vacuo* to give a large amount of white powder. This was dissolved in a minimum amount of warm water (~ 6 mL) and a solution of $NH_4PF_6$ (0.2 g) in water (1 mL) was added. Leaving this to stand overnight in a refrigerator[1] gave colourless crystals, which were isolated by filtration, washed with water (4 × 2 mL) and dried *in vacuo*. $^1$H, $^{19}$F and $^{31}$P NMR spectroscopy indicated that these crystals were pure $\mathbf{BB{\cdot}4PF_6}$ (Figures S16–S18). Yield: 7 mg (6 μmol, ~ 60%). Mass spectrometry showed peaks at m/z = 955.5 (calc. for $[\mathbf{BB{\cdot}3PF_6}]^+$ = 955.1) and 405.2 (calc. for $[\mathbf{BB{\cdot}2PF_6}]^{2+}$ = 405.1).

[1] When $\mathbf{BB{\cdot}4PF_6}$ is prepared normally, precipitation occurs instantly on addition of excess $NH_4PF_6$. In this case there is a very small amount of $\mathbf{BB^{4+}}$ relative to the large amount of $NH_4Cl$ used to extract it, hence the slower crystallization.

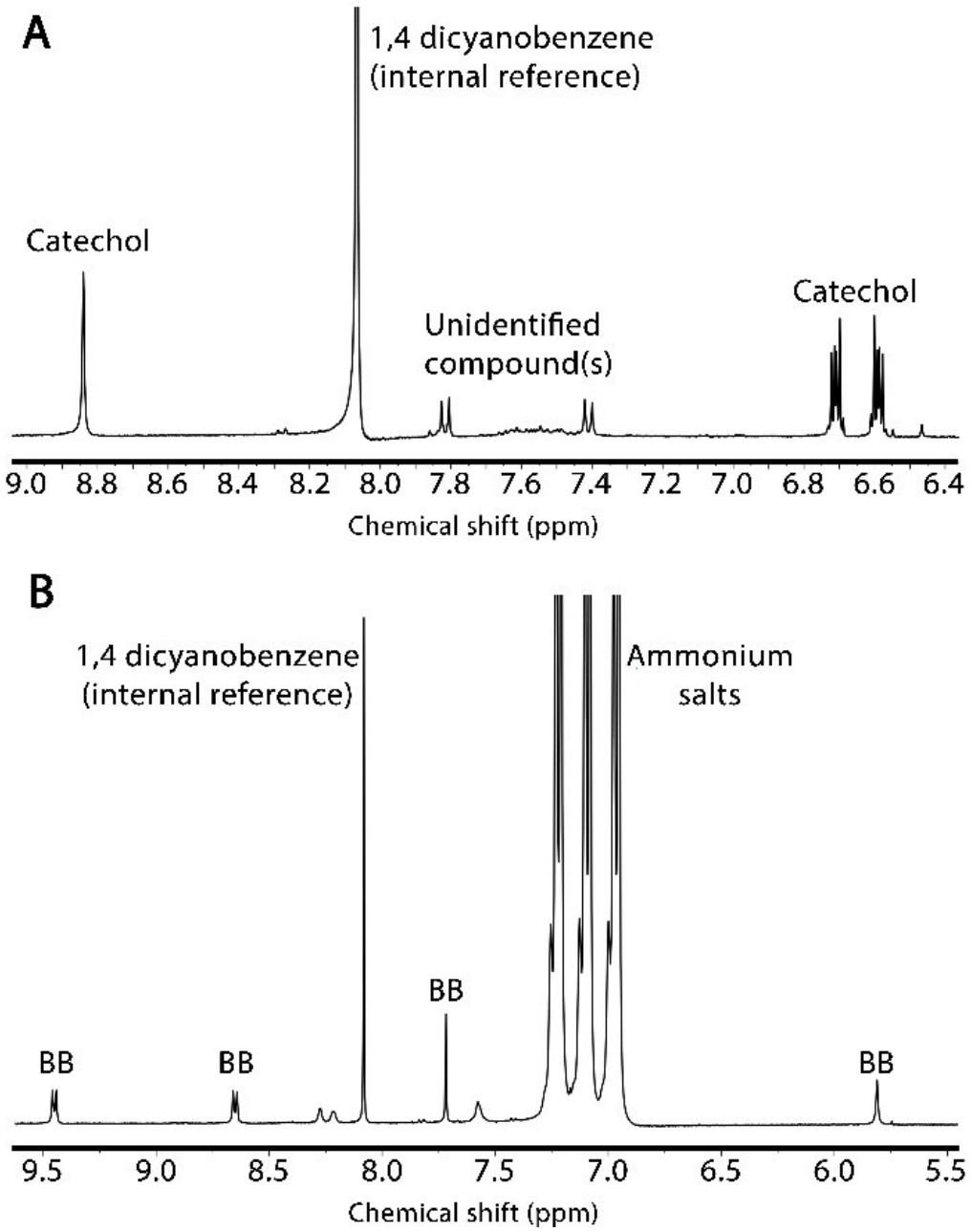


**Figure S16**: $^{1}$H NMR spectrum (298 K, 400 MHz, $d_6$-DMSO) of A: methanol/dichloromethane extract from BB-functionalized silica; B: methanol/water/sat. aq. $NH_4Cl$ extract from BB-functionalized silica after subsequent extraction into acetonitrile in the presence of TBA·$PF_6$.

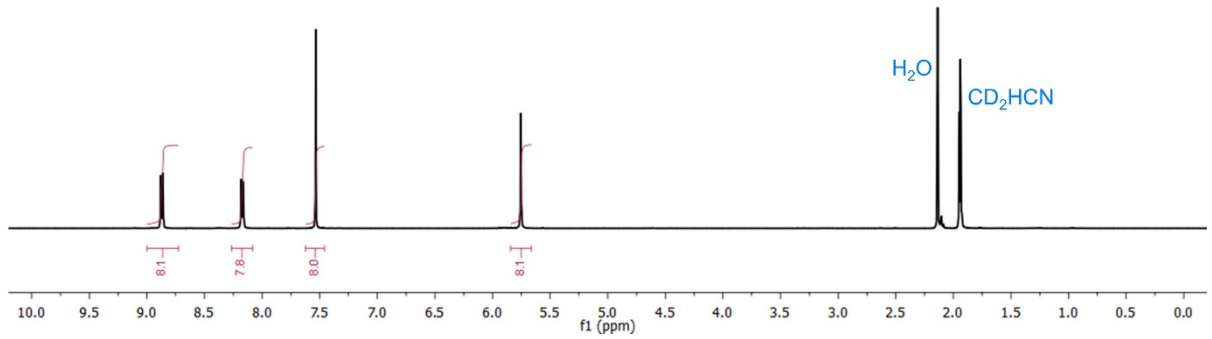


**Figure S17.** $^{1}$H NMR spectrum of pure **BB·4PF$_6$** recovered from silica powder after catechol polymerization experiments (298 K, 400 MHz, $CD_3CN$).

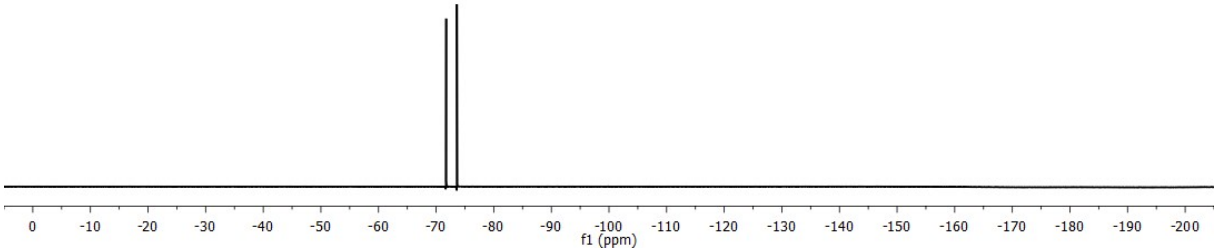


**Figure S18.** $^{19}$F NMR spectrum of pure **BB·4PF$_6$** recovered from silica powder after catechol polymerization experiments (298 K, 376 MHz, $CD_3CN$).

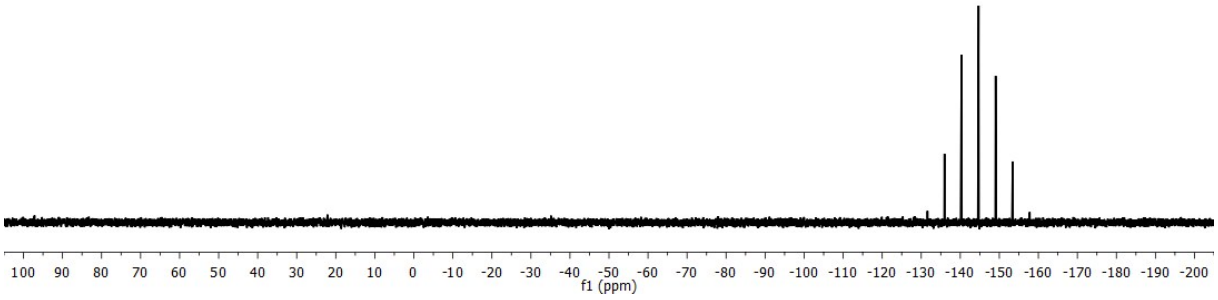


**Figure S19.** $^{31}$P NMR spectrum of pure **BB·4PF$_6$** recovered from silica powder after catechol polymerization experiments (298 K, 162 MHz, $CD_3CN$).

## SI References

1. P. R. Ashton, B. Odell, M. V. Reddington, A. M. Z. Slawin, J. F. Stoddart and D. J. Williams, *Angewandte Chemie International Edition in English*, 1988, **27**, 1550-1553.
2. J. Cosier and A. M. Glazer, *J. Appl. Crystallogr.*, 1986, **19**, 105-107.

3. *CrysAlisPro*, Agilent Technologies, 2011.
4. A. Altomare, G. Cascarano, C. Giacovazzo, A. Guagliardi, M. C. Burla, G. Polidori and M. Camalli, *J. Appl. Crystallogr.*, 1994, **27**, 435-436.
5. P. W. Betteridge, J. R. Carruthers, R. I. Cooper, K. Prout and D. J. Watkin, *J. Appl. Crystallogr.*, 2003, **36**, 1487.
6. R. I. Cooper, A. L. Thompson and D. J. Watkin, *J. Appl. Crystallogr.*, 2010, **43**, 1100-1107.
7. *Bindfit software, supramolecular.org*, 2018, **2018**.